

Fig. S1. Validation of MS Screen and additional RHBDL4 substrate candidates. (A) Hek293 T-REx cells stably express C-terminally GFP tagged RHBDL4 (R4-GFP) wt, catalytically inactive SA or catalytically inactive RHBDL4 with an additional mutated UIM (SAUM) upon induction with doxycycline (dox). WB, western blot. (B) Hek293T cells transiently transfected with empty vector (-), R4-GFP wt, the catalytically inactive SA mutant or the SAUM double mutant were lysed with Triton X-100 and subjected to GFP-specific immunoprecipitation (IP). Western blots (WB) analysis reveals increased co-purification of endogenous RPN1 and STT3A. (C) Outline of N-terminally FLAG-tagged FLAG-RPN2, FLAG-DDOST and FLAG-B4GAT1 constructs used in this study. Numbers indicate position of TM domain boundaries. (D) Hek293T cells were co-transfected with FLAG-RPN2 and either an empty vector (-), N-terminally HA-tagged RHBDL4 (HA-R4) wt or the catalytically inactive SA mutant. RHBDL4 generates N-terminal cleavage fragments (open triangle) that are degraded by the proteasome as shown by increased steady state level upon MG132 treatment (2 μ M) compared to vehicle control (DMSO). (E) Cleavage assay as shown in (D) but with FLAG-DDOST as substrate. (F) Cleavage assay as shown in (D) but with FLAG-B4GAT1 as substrate.

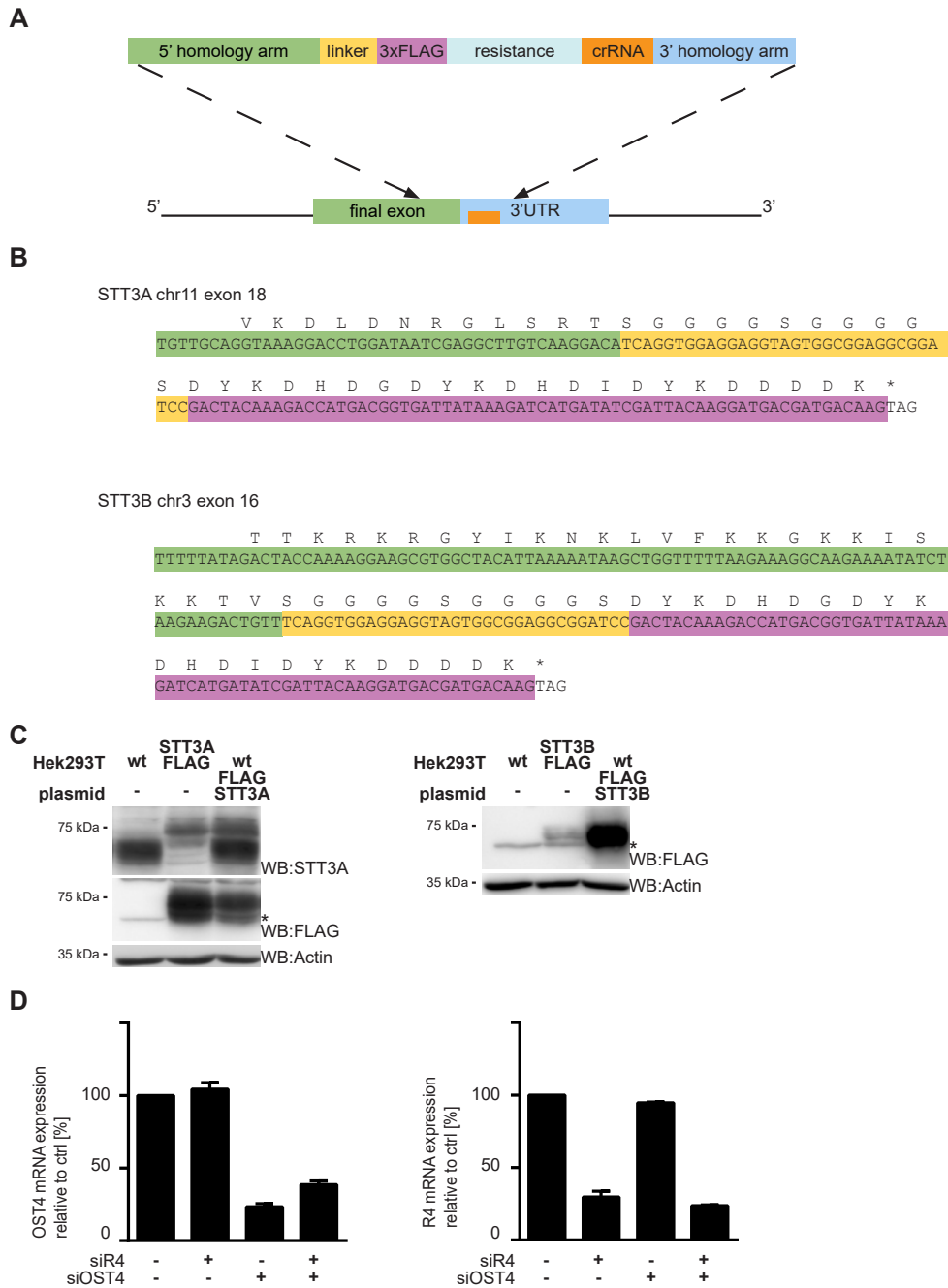


Fig. S2. Endogenously tagged STT3A and STT3B. (A) Outline of the applied tagging strategy according to (Fueller et al., 2019). (B) Sanger sequencing of chromosomal DNA obtained from the indicated Hek293T cell lines shows insertion of the triple-FLAG tag in the last coding exon. Color code as in (A). (C) Western blot (WB) analysis of endogenous STT3A, chromosomally tagged STT3A-FLAG and ectopically expressed FLAG-STT3A (left) and WB analysis of chromosomally tagged STT3B-FLAG and ectopically expressed FLAG-STT3B (right) from total cell lysates from Hek293T wt or HEK293T cell line with endogenously tagged STT3A or STT3B, respectively. Empty Vector transfected (-). Ectopic expression of FLAG-STT3A (from 1 μ g plasmid) leads to steady state level comparable to the endogenously tagged STT3A-FLAG. 0.5 μ g plasmid encoding FLAG-STT3B leads to overexpression as judged by the FLAG-signal. Of note, no STT3B-specific antibody was available restricting the analysis to FLAG-tag. Actin levels are shown as loading control. Asterisk, unspecific band. (D) Transcriptional levels of OST4 and RHBDL4 in HEK293T wt cells of an experiment as shown in Fig. 2A and B relative to sictrl. Normalized to the arithmetic mean of the housekeeping genes β -2 microglobulin and TATA-binding protein.

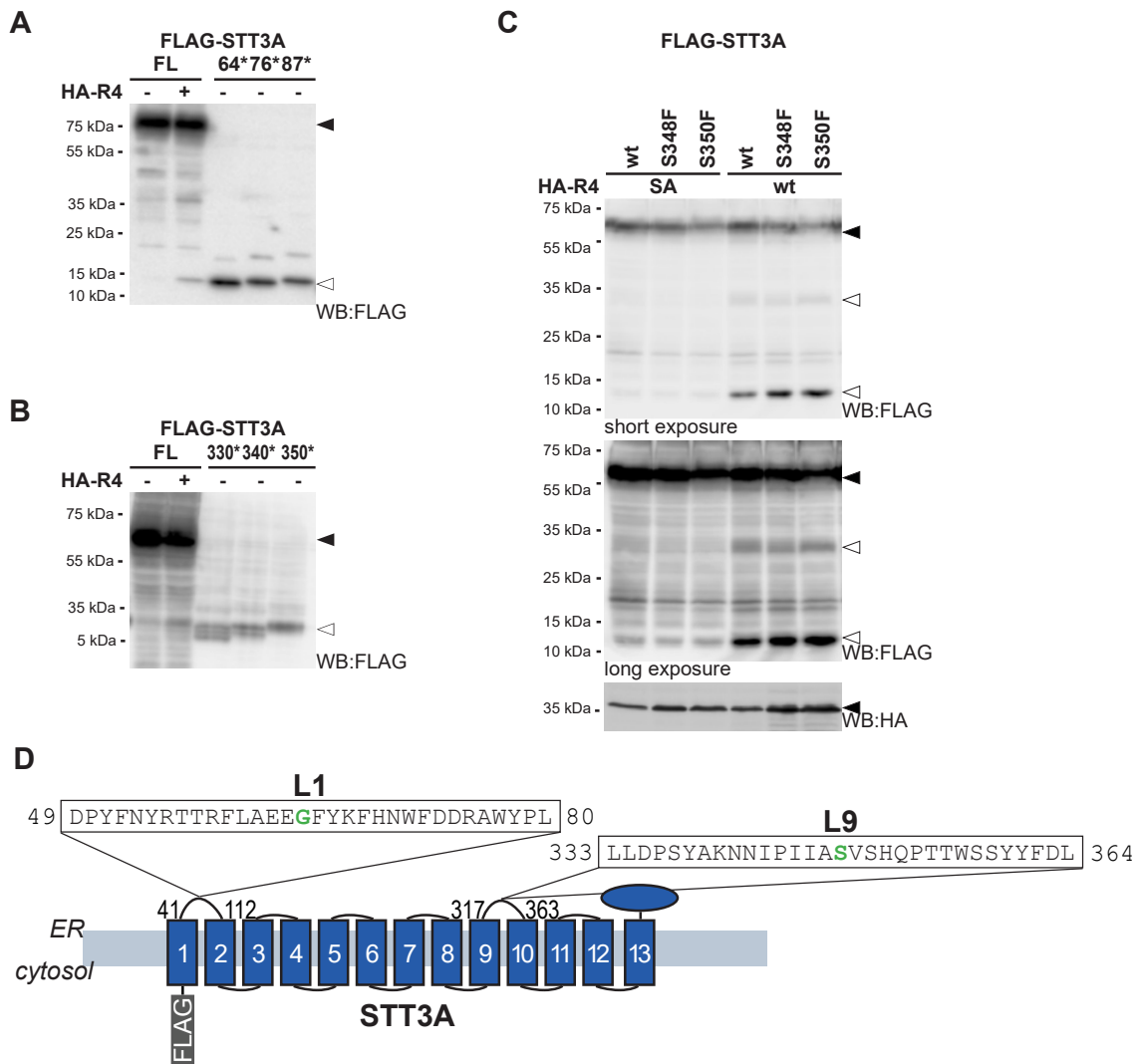


Fig. S3. STT3A is cleaved within two distinct luminal loops. (A) Hek293T cells were transfected with full-length (FL) FLAG-STT3A and either an empty vector (-) or HA-tagged RHBDL4 (HA-R4). In addition, cells were transfected with FLAG-STT3A variants truncated at position 64 (64*), 76 (76*) and 87 (87*). Open triangle highlights RHBDL4 generated cleavage fragment at 13 kDa. Cells have been treated with MG132 (2 μ M). WB, western blot. (B) Assay as in (A) but FLAG-STT3 with truncations after amino acid 330, 340 and 350 have been used as reference peptides. (C) Hek293T cells were transfected with FLAG-STT3A wt, or with S348F, or a S350F mutant of FLAG-STT3A (filled triangle) together with either the catalytically inactive SA mutant or HA-tagged RHBDL4 (HA-R4) constructs as indicated. Overexpression of the active rhomboid (wt) resulted in cleavage fragments at 35 kDa (L9) and 13 kDa (L1) (open triangles) observed significantly less for the SA mutant. In order to prevent clearance of cleavage fragments, cells have been treated with proteasome inhibitor MG132 (2 μ M). (D) Outline of luminal STT3A sequences flanking the predicted RHBDL4 cleavage sites at G64 and S348. Numbers indicate position of TM domain boundaries.

A

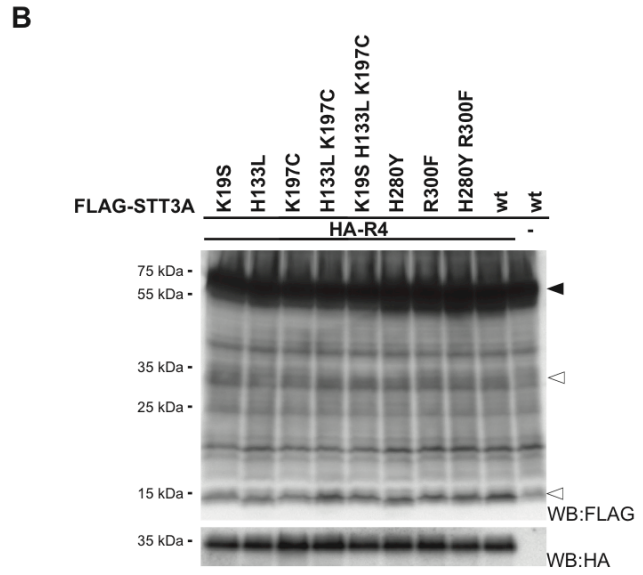
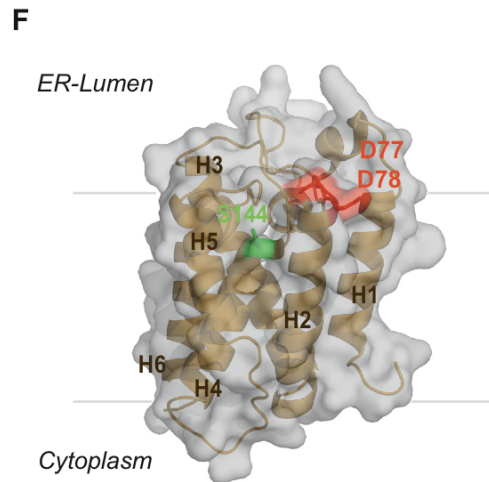
TMD1	STT3A	LLKLLLLLSMAAVLSFSTR ^L FAVLR ^F
	STT3B	LLSFTILFLAWLAGFSS ^R LFAVIR ^F
TMD2	STT3A	IRNVCVFLAPL ^F SSFTTIVTY ^H LTK ^R
	STT3B	IRDVCVFLAPTF ^F SGLTSISTFLL ^R
TMD3	STT3A	DAGAGLLAAAMI ^A VVPGYIS ^R
	STT3B	NQGAGLLAAC ^F IAIVPGYIS ^R
TMD4	STT3A	IAIFCMLLYYMWIK ^A VK ^K
	STT3B	IAIFALQFTYYLWV ^K SVK ^K
TMD5	STT3A	SICWAA ^K CALAYFYMVSSW
	STT3B	SVFWTMCCLSYFYMVSAW
TMD6	STT3A	GYVFLINLIPL ^H VLVLM ^L T
	STT3B	GVVFIINLIPL ^H VFVLL ^L M
TMD7	STT3A	SHRIYVAYCTVYCLGTILSMQ
	STT3B	SKRVYIAYSTFYIVGLILSMQ
TMD8	STT3A	SSEHMAAFGVFGLCQI ^H AFVDYL
	STT3B	TSEHMAAGVFALLQAYAF ^L QYL
TMD9	STT3A	QFEVLF ^R SVISLVGFVLLTVGALL
	STT3B	EFQTLFFLGVSLAAGAV ^F LSVIYL
TMD10	STT3A	LQLLVFMFPVGLYCF ^S N
	STT3B	LHILVCTFPAGLW ^F CI ^K N
TMD11	STT3A	ARIFIIMYGVTSMY ^F S
	STT3B	ERVFVALYAI ^S AVY ^F FA
TMD12	STT3A	VR ^L MLVLAPVMCILSGIGVQVLSTYM
	STT3B	VR ^L MLTLTPVVCMLSAIAF ^S NVFE ^H YL
TMD13	STT3A	VASGMILVMAFFLITYTF ^H STWV
	STT3B	IK ^S IVTMLMLMLLMF ^A VH ^C TWV

C

TMD1	RPN2	VSNTFTALILSPL ^L LLFALWI
TMD2	RPN2	FAPSTII ^F H ^L GHAA ^M LGLMYV
TMD3	RPN2	LNM ^F QTL ^K YLAILG ^S VTFLAG

D

TMD	RPN1	PLL ^V VAAFYILF ^F TVII ^Y V
TMD	DDOST	YYASAFS ^M MLGL ^F IFSIV ^F L
TMD	B3GNT1	CAFYQL ^L LAALMLV ^A MLQ ^L LYL ^S LLSGL



E

Hec GlpG_P09391	HFSLM ^H IL ^F NLL ^L WWYL ^L GGAVE ^K R
Hs RHBDL1_Q75783	HVGLE ^Q LGF ^N ALL ^L QLMIGV ^P LEMV
Hs RHBDL2_Q9NX52	HAGVQ ^H IL ^G NLC ^M QLVL ^G I ^P LEMV
Hs RHBDL3_P58872	HAGIE ^H LGL ^N VVL ^L QLLV ^G V ^P LEMV
Mm RHBDL1_Q8VC82	HVGLE ^Q LGF ^N ALL ^L QLMIGV ^P LEMV
Mm RHBDL2_A2AGA4	HAGVQ ^H I ^V GNLL ^M QI ^V L ^G I ^P LEMV
Mm RHBDL3_P58873	HAGVE ^Q LGL ^N VAL ^L QLLV ^G V ^P LEMV
Dr RHBDL1_E7FCU6	HVGLE ^Q LGF ^N ALL ^L QLMIGV ^P LEMV
Dr RHBDL2_Q7ZUN9	HAGVE ^H IMGNLL ^M QLL ^L GI ^P LELV
Dr RHBDL3_Q566N3	HAGIE ^H LGL ^N MAM ^Q LLV ^G V ^P LEMV
consensus A-type	* . * : : : * * : * : : * : : * : *
Hs RHBDL4_Q8TEB9	HADD ^W H ^L Y ^F NMAS ^L MLW ^K GIN ^L ERR
Mm RHBDL4_Q8BHC7	HGDD ^W H ^L Y ^F NM ^S MSLW ^K GV ^K LERR
Dr RHBDL4_Q568J3	HVDD ^W H ^L Y ^F NM ^A LLW ^K GIR ^L EKK
consensus B-type	* *
consensus total	* . . : : * * * * * * * * * *

A-type
B-type

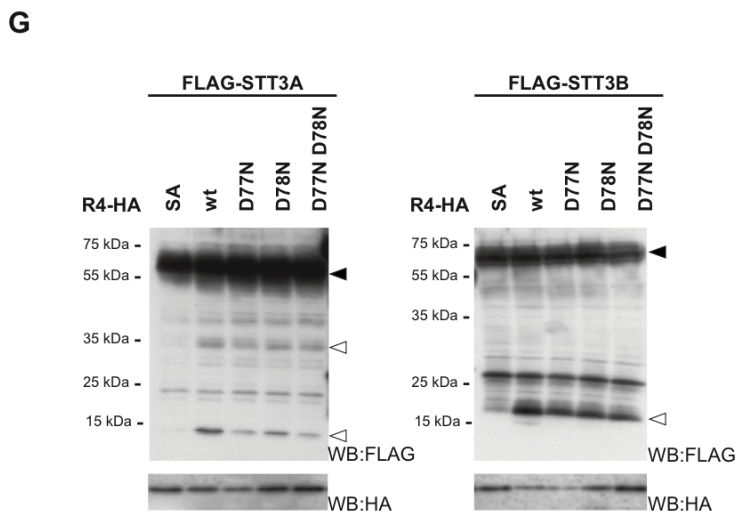


Fig. S4. STT3A and STT3B show differently charged TM Domains. (A) Alignment of STT3A and STT3B TM domains (TMD). Positive charged residues are highlighted in blue. Positive charges in STT3A TMDs absent in STT3B are highlighted in yellow. (B) FLAG-STT3A wt or FLAG-STT3A with positive charged TMD residues replaced as indicated with the respective residues of STT3B, have been transfected either with empty vector (-) or HA-tagged RHBDL4 (HA-R4) and cells have been treated with MG132 (2 μ M). WB, western blot. (C) RPN2 TMDs. Positive charged residues are highlighted in blue. (D) TMDs of RPN1, DDOST and B4GAT1. (E) Multiple-sequence alignment of TM segment H2 from *E. coli* (Ec) GlpG and secretory pathway rhomboids from human (*H. sapiens*, Hs), mouse (*M. musculus*, Mm) and *D. rerio* (Dr) shows two conserved aspartate residues D77/D78 (highlighted in red) that are missing in the other RHBDLs. Sequence consensus of the A-class and B-class secretase rhomboids according to (Lemberg and Freeman, 2007) are shown. Functionally important residues forming the putative oxyanion hole important for catalysis are highlighted in green (Strisovsky, 2016). (F) Homology model of RHBDL4 reveals position of the putative negative charged substrate docking site. Position of the active site serine-144 (S144) in the active site groove and aspartate-77 (D77) and aspartate-78 (D78) in the putative gating TM segment H2 (Cho et al., 2019) are indicated. (G) Hek293T cells were transfected with FLAG-STT3A or FLAG-STT3B (filled triangle) together with either RHBDL4 SA, wt or RHBDL4 variants where negative charged aspartate residues have been replaced by uncharged asparagines (D77N, D78N, D77N/D78N). RHBDL4 generated cleavage fragments at 13 kDa and 35 kDa for STT3A and at 16 kDa for STT3B are highlighted by open triangles. Cells have been treated with MG132 (2 μ M). See Fig. 5D for quantification.

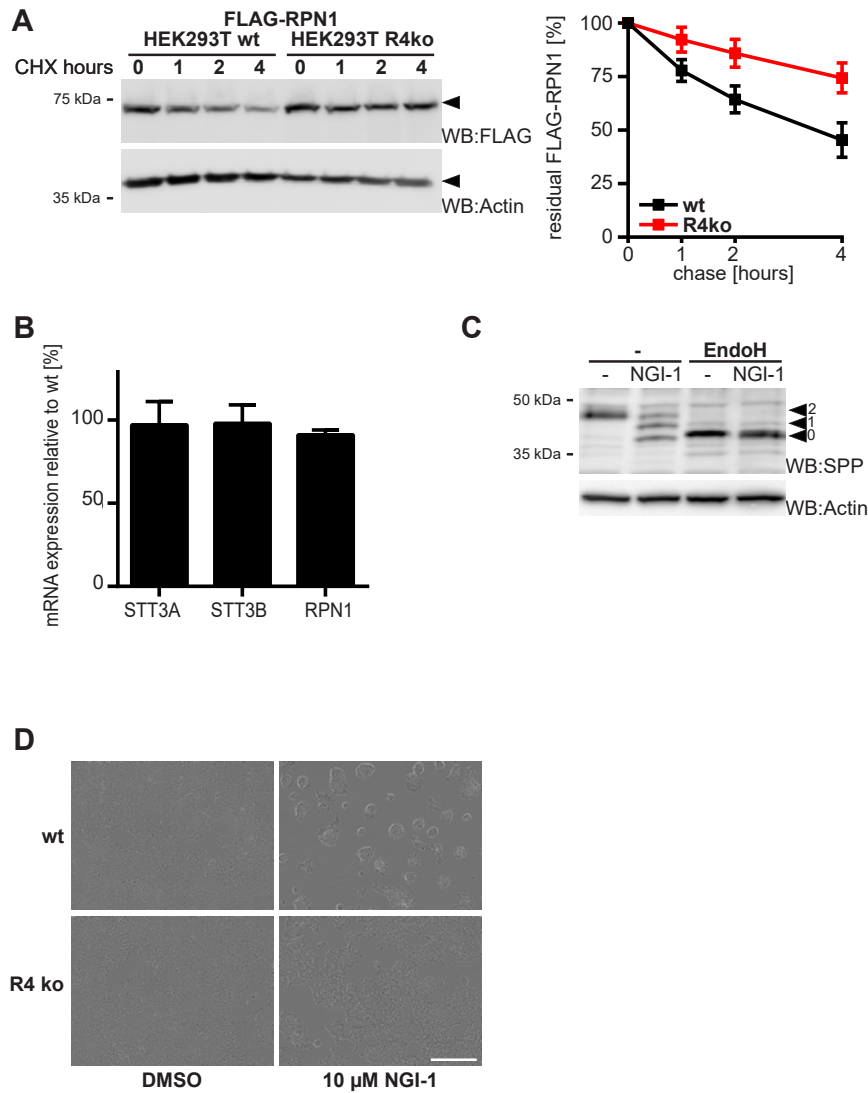


Fig. S5. Functional characterization of RHBDL4 knockout cells. (A) Hek293T cells, either wt or RHBDL4 knock-out (R4ko) transiently expressing FLAG tagged RPN1 (FLAG-RPN1) were subjected to cycloheximide (CHX) chase and analyzed by western blotting (WB). Actin serves as loading control. Right panel: Quantification of RPN1-FLAG expression level relative to respective timepoint 0 (means \pm SEM, n=3). (B) Transcriptional levels of STT3A, STT3B and RPN1 in HEK293T R4ko cells relative to Hek293T wt cells normalized to the arithmetic mean of the housekeeping genes β -2 microglobulin and TATA-binding protein. (C) Glycosylation status of SPP in Hek293T cells after treatment with DMSO or 10 μ M NGI-1 for 24 h analyzed by WB. NGI-1-treatment results in appearance of mono and unglycosylated SPP. Treatment with Endo H removes all N-linked glycans. (D) Images of the cells treated with OST inhibitor NGI-1 or vehicle control (DMSO) depicted in Fig. 6D. 10-fold magnification of cells 60 hours after start of the growth curve. Scale bar: 400 μ m.

Table S1. Complete list of proteins identified by RHBDL4 substrate trapping MS/MS.
See separate file.

Table S2. Substrate Candidates identified by RHBDL4 substrate trapping MS/MS.

Table S1 selected for the following criteria: quantified in both replicates, ≥ 2 unique peptides, GO term “integral to membrane” and “endoplasmic reticulum”, mean Heavy over Light ratio ≤ 2.0 . Number of transmembrane domains has been added manually.

Table S3. Proteins identified by protein pilot search to determine sequons for N-linked glycosylation – Protein Summary.

See separate file.

Table S4. Proteins identified by protein pilot search to determine sequons for N-linked glycosylation – Peptide Summary.

See separate file.

Table S5. Proteins identified by protein pilot search to determine sequons for N-linked glycosylation – Distinct Peptide Summary.

See separate file.

Table S6. Ratios of site-specific N-linked occupancy for partially occupied sequons.

See separate file.